TÜBİTAK

Turkish Journal of Chemistry

http://journals.tubitak.gov.tr/chem/

Research Article

Turk J Chem
(2022) 46: 786-795

10.55730/1300-0527.3368

Synthesis and in vitro α-glucosidase and cholinesterases inhibitory actions of water-soluble metallophthalocyanines bearing ({6-[3-(diethylamino)phenoxy]hexyl}oxy groups

Turgut KELEŞ[1], Zekeriya BIYIKLIOĞLU[2,*], Didem AKKAYA[3], Arzu ÖZEL[3], Burak BARUT[3]

[1]Central Research Laboratory Application and Research Center, Recep Tayyip Erdoğan University, Rize, Turkey
[2]Department of Chemistry, Faculty of Science, Karadeniz Technical University, Trabzon, Turkey
[3]Department of Biochemistry, Faculty of Pharmacy, Karadeniz Technical University, Trabzon, Turkey

Received: 24.11.2021 • **Accepted/Published Online:** 18.01.2022 • **Final Version:** 16.06.2022

Abstract: In this paper, we have prepared peripherally tetra-({6-[3-(diethylamino)phenoxy]hexyl}oxy substituted cobalt(II), copper(II), manganese(III) phthalocyanines (**3, 4, 5**) and their water-soluble derivatives (**3a, 4a, 5a**). Then, in vitro α-glucosidase and cholinesterases inhibitory actions of the water-soluble **3a, 4a, 5a** were examined using spectrophotometric methods. **4a** had the highest inhibitory effects among the tested compounds against α-glucosidase due to IC_{50} values. **4a** and **5a** had 40 fold higher inhibitory effects than the positive control. For cholinesterases, the compounds showed significant inhibitory actions that of galantamine which was used as a positive control. According to the SI value, **3a** inhibited acetylcholinesterase enzyme selectively. In kinetic studies, **4a** was a mixed inhibitor for α-glucosidase, **3a** was a competitive inhibitor for AChE, and **4a** was a mixed inhibitor for BuChE. The therapeutic potential of these compounds has been demonstrated by in vitro studies, but these data should be supported by further studies.

Key words: Phthalocyanine, water-soluble, cholinesterases, α-Glucosidase, enzyme kinetic

1. Introduction

Diabetes Mellitus (DM), which is a metabolic disease that occurs in advanced ages and is characterized by hyperglycemia, causes health complications such as retinopathy, nephropathy, cardiovascular disease, and obesity [1,2]. Controlling hyperglycemia and regulating blood sugar levels are the most important targets for this metabolic disease [3,4]. One of the most important approaches used in the treatment of DM is the inhibition of the α-glucosidase enzyme, which breaks down polysaccharides into smaller saccharides. With the inhibition of α-glucosidase, the hydrolysis of food-derived sugar is prevented, thereby controlling the blood sugar level and regulating postprandial hyperglycemia [5,6]. Although α-glucosidase inhibitors such as acarbose, miglitol, and voglibose are currently used in the treatment, various side effects such as nausea, diarrhea, and gastrointestinal discomfort are observed in the clinic [7,8]. The search for alternative α-glucosidase inhibitors to these drugs, which are less costly and have fewer side effects, continues [9,10].

Alzheimer's disease (AD), is one of the neurodegenerative diseases that progresses over time and has limited treatment [11,12]. This disease causes memory, learning loss, and selective/irreversible impairments that occur in cholinergic function. This is called the "cholinergic hypothesis" in the pathogenesis of AD [13,14]. Acetylcholinesterase (AChE) and butyrylcholinesterase (BuChE) enzymes, which are responsible for the termination of the neurotransmission signal in the cholinergic hypothesis associated with learning and memory function, perform this task by hydrolyzing acetylcholine (ACh) to choline and acetic acid. Low ACh levels are a condition that should be treated in AD [15,16]. Today, cholinesterase (ChE) inhibitors such as galantamine, rivastigmine, donepezil, and tacrine are used for AD in clinic. However, its clinical usage has been limited due to various side effects such as hepatotoxicity, gastrointestinal system disorders, and hypotension arising [17,18].

Phthalocyanines have been used in various biological and industrial areas such as photodynamic therapy [19], anticancer agents [20], organic photovoltaic devices [21], liquid crystals [22], electrochromic display devices [23], solar cell [24], electrocatalytic agents [25] owing to their chemical and physical properties. Also, there are many studies on the α-glucosidase and cholinesterase inhibitory effects of phthalocyanines in the literature [26,27]. Diethylamino groups are widely preferred as substituted groups on water-soluble phthalocyanines, as they have both biological and pharmacological importance and contain nitrogen atoms that can be quaternized [28,29]. For this reason, the aim of this

* Correspondence: zekeriyab@ktu.edu.tr

study is to determine the in vitro α-glucosidase and cholinesterases inhibitory effects of water-soluble cobalt(II), copper(II), manganese(III) phthalocyanines bearing peripherally tetra-({6-[3-(diethylamino)phenoxy]hexyl}oxy groups.

2. Experimental

The used materials, equipment, and in vitro inhibition assay on α-glucosidase, AChE, and BuChE are given in supplementary information.

2.1. Synthesis

2.1.1. 4-({6-[3-(Diethylamino)phenoxy]hexyl}oxy)phthalonitrile (2)

6-[3-(Diethylamino)phenoxy]hexan-1-ol **(1)** (1 g, 3.78 mmol), 4-nitrophthalonitrile (0.65 g, 3.78 mmol), dry K_2CO_3 (1.6 g, 11.34 mmol) were dissolved in DMF (15 mL) at 60 °C under N_2 atmosphere for 4 days. Then, reaction mixture was poured into water (200 mL) and stirred for 3 h. After that, the aqueous phase extracted with chloroform (3 × 50 mL). The combined extracts were dried over anhydrous $MgSO_4$ and then filtered. The product was purified by aluminum oxide column chromatography using $CHCl_3$. Yield: 0.5 g (34%). IR (ATR), ν/cm^{-1}: 3075 (Ar–H), 2942–2870 (Aliph. C–H), 2230 (C ≡ N), 1598, 1501, 1473, 1394, 1315, 1281, 1255, 1213, 1169, 1096, 1022, 919, 803, 758. ^{1}H NMR (400 MHz, DMSO-d_6), (δ): 8.01 (d, 1H, Ar-H), 7.72 (s, 1H, Ar–H), 7.42 (d, 1H, Ar–H), 6.98 (t, 1H, Ar–H), 6.22 (d, 1H, Ar–H), 6.12–6.08 (m, 2H, Ar-H), 4.11 (t, 2H, CH_2–O), 3.88 (t, 2H, CH_2–O), 3.28–3.23 (q, 4H, –CH_2-N), 1.73–1.66 (m, 4H, –CH_2-), 1.45–1.39 (m, 4H, –CH_2-), 1.05 (t, 6H, CH_3). ^{13}C-NMR (100 MHz, DMSO-d_6), (δ): 162.48, 160.39, 149.14, 136.16, 130.19, 120.66, 120.46, 116.70, 116.68, 116.17, 106.16, 105.00, 101.20, 98.61, 69.41, 67.30, 44.09, 29.19, 28.61, 25.69, 25.52, 12.88. MS (ESI), (*m/z*) calcd. 391.50; found: 391.70 [M]$^+$.

2.1.2. The synthesis procedure of metallophthalocyanines (3, 4, 5)

4-({6-[3-(Diethylamino)phenoxy]hexyl}oxy)phthalonitrile **(2)** (100 mg, 0.25 mmol), 0.12 mmol related metal salts (16 mg $CoCl_2$, 16 mg $CuCl_2$, 17 mg $MnCl_2$) in 1-pentanol (2 mL) and 1,8-diazabycyclo [5.4.0]undec-7-ene (DBU) (3 drops) was heated at 160 °C for 1 day. The product was precipitated with *n*-hexane. Finally, (**3, 4, 5**) were purified by aluminum oxide column chromatography using $CHCl_3$.

2.1.3. Cobalt(II) phthalocyanine (3)

Yield: 20 mg (20%), m.p. >250 °C. IR (ATR), ν/cm^{-1}: 3066 (Ar–H), 2920–2850 (Aliph. C–H), 1729, 1607, 11497, 1488, 1467, 1357, 1232, 1214, 1178, 1094, 820, 748, 654. UV–Vis (DMF) λmax nm (log ε): 668 (4.93), 609 (4.51), 328 (4.92). MALDI-TOF-MS m/z calc. 1624.95; found: 1624.56 [M]$^+$.

2.1.4. Copper(II) phthalocyanine (4)

Yield: 26 mg (26%), m.p. > 250 °C. IR (ATR), ν/cm^{-1}: 3071-3038 (Ar–H), 2968–2855 (Aliph. C–H), 1607, 1570, 1498, 1465, 1388, 1343, 1238, 1214, 1119, 1093, 956, 820, 745, 687. UV–Vis (DMF) λmax nm (log ε): 680 (5.02), 617 (4.679), 341 (4.86). MALDI-TOF-MS m/z calc. 1629.57; found: 1629.28 [M]$^+$.

2.1.5. Manganese(III) phthalocyanine chloride (5)

Yield: 50 mg (47%), m.p. > 250 °C. IR (ATR), ν/cm^{-1}: 3071 (Ar–H), 2926–2858 (Aliph. C–H), 1603, 1496, 1464, 1341, 1240, 1214, 1123, 1074, 1052, 821, 745, 686. UV–Vis (DMF) λmax nm (log ε): 729 (4.98), 652 (4.59), 500 (4.36), 355 (4.85). MALDI-TOF-MS m/z calc. 1656.41; found: 1621.35 [M-Cl]$^+$.

2.1.6. The synthesis procedure of water-soluble metallophthalocyanines (3a, 4a, 5a)

3a (20 mg, 0.012 mmol), **4a** (20 mg, 0.016 mmol), **5a** (20 mg, 0.012 mmol) was dissolved in $CHCl_3$ (2.5 mL), added iodomethane (2 mL) and stirred at rt for 4 days. The precipitated products were filtered and washed with $CHCl_3$, diethyl ether.

2.1.7. Water-soluble cobalt(II) phthalocyanine (3a)

Yield: 19 mg (70%), m.p. > 250 °C. IR (ATR), ν/cm^{-1}: 3061 (Ar–H), 2932–2859 (Aliph. C–H), 1713, 1606, 1456, 1408, 1337, 1231, 1116, 1092, 1060, 1006, 870, 823, 750. UV-Vis (DMF), λ_{maks} (loge) nm : 671 (4.94), 608 (4.48), 327 (4.85). MALDI-TOF-MS m/z calc. 2192.71; found: 421.12 [M-4I]$^{+4}$.

2.1.8. Water-soluble copper(II) phthalocyanine (4a)

Yield: 20 mg (74%), m.p. > 250 °C. IR (ATR), ν/cm^{-1}: 3013 (Ar–H), 2934–2860 (Aliph. C–H), 1607, 1487, 1457, 1390, 1232, 1090, 1053, 1005, 870, 745, 689. UV-Vis (DMF), λ_{maks} (loge) nm : 680 (5.03), 612 (4.44), 345 (4.70). MALDI-TOF-MS m/z calc. 2197.32; found: 422.24 [M-4I]$^{+4}$.

2.1.9. Water-soluble manganese(III) phthalocyanine chloride (5a)

Yield: 17 mg (65%), m.p. > 250 °C. IR (ATR), ν/cm^{-1}: 3019 (Ar–H), 2933–2860 (Aliph. C–H), 1602, 1457, 1391, 1338, 1235, 1119, 1054, 993, 1054, 999, 869, 745, 691. UV-Vis (DMF), λ_{maks} (loge) nm : 728 (5.01), 661 (4.55), 500 (4.37), 367 (4.85). MALDI-TOF-MS m/z calc. 2224.17; found: 420.12 [M-Cl-4I]$^{+4}$.

3. Results and discussion

3.1. Synthesis and characterization

The synthesis of peripherally tetra-({6-[3-(diethylamino)phenoxy]hexyl}oxy) group substituted metallophthalocyanines and their water-soluble derivatives are given in Figure 1 and 2. 4-({6-[3-(Diethylamino)phenoxy]hexyl}oxy)phthalonitrile (**2**) was prepared by the reaction of 6-[3-(diethylamino)phenoxy]hexan-1-ol (**1**) [30] and 4-nitrophthalonitrile in DMF at 60 °C. Cobalt(II), copper(II), and manganese(III) phthalocyanines (**3, 4, 5**) were synthesized by reaction of **2** and metal salts in 1-pentanol. Then, water-soluble phthalocyanines (**3a, 4a, 5a**) were prepared by reaction of cobalt(II), copper(II), and manganese(III) phthalocyanines (**3, 4, 5**) with iodomethane at room temperature [31,32]. In the IR spectrum of **2**, the new vibration belonging to C ≡ N group appeared as expected. In the ^{1}H-NMR spectrum of **2,** aromatic protons were observed at δ 8.01–6.08 ppm. Also, CH_2–O (4.11, 3.88 ppm), CH_2-N (3.28-3.23), and –CH_3 (1.05 ppm) protons were seen as expected. In the ^{13}C-NMR spectrum of **2**, the nitrile group of carbon atom resonances was seen between 116.70

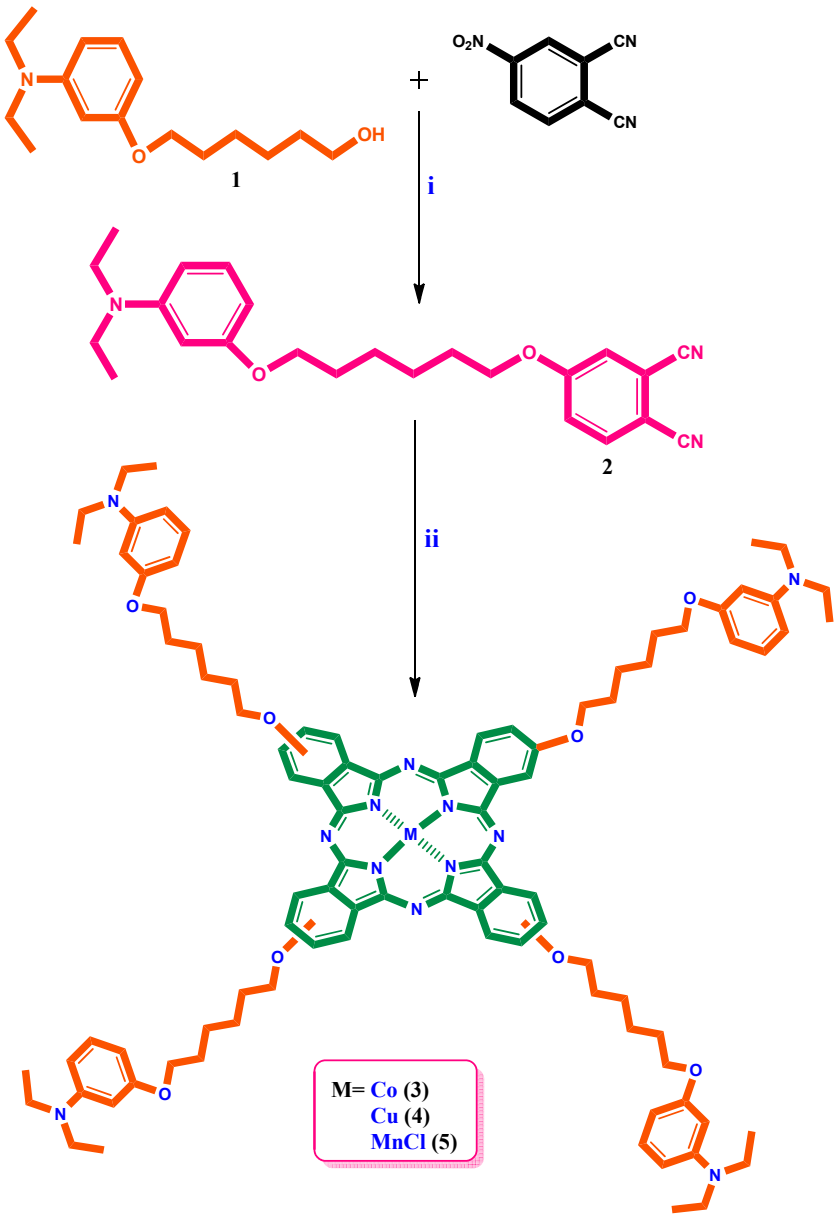

Figure 1. Synthesis of metallophthalocyanines. (i) K_2CO_3, 60 °C, DMF. (ii) $CoCl_2$, $CuCl_2$, $MnCl_2$, 1-pentanol, DBU, 160 °C.

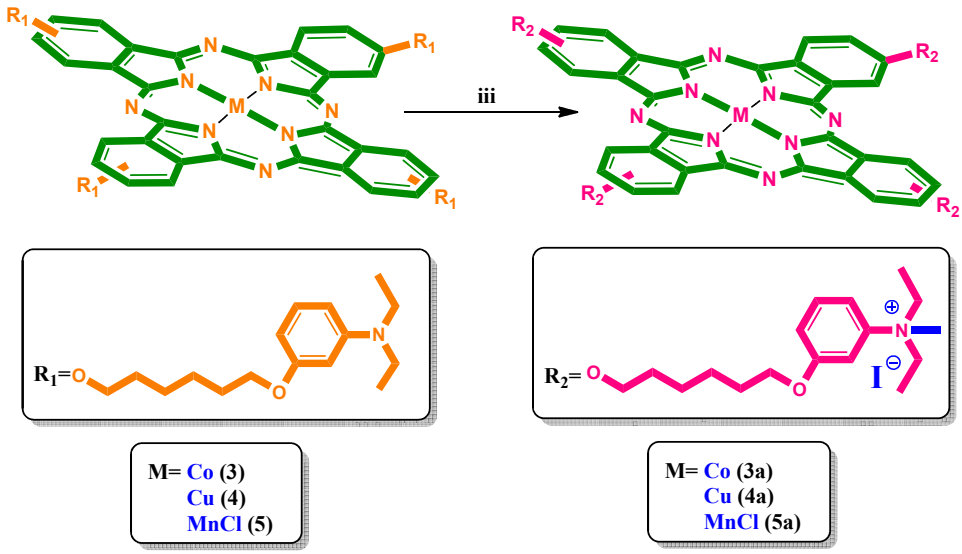

Figure 2. Synthesis of water-soluble phthalocyanines. (iii) $CHCl_3$, CH_3-I, rt.

and 116.17 ppm. In the mass spectrum of 4-({6-[3-(diethylamino)phenoxy]hexyl}oxy)phthalonitrile (**2**), the $[M]^+$ peak at 391.70 verified the suggested structure. In the IR spectra of (**3, 4, 5**), the sharp –C ≡ N vibrations of **2** disappeared as expected. The ^{1}H-NMR spectra of (**3, 4, 5**) could not be recorded due to the paramagnetic metal ions in the ring center [33]. Also, the IR spectra of (**3a, 4a, 5a**) were very similar to (**3, 4, 5**). In the MALDI–TOF–MS of (**3, 4, 5**) the presence of the molecular ion peaks at m/z = 1624.56 $[M]^+$, m/z = 1629.28 $[M]^+$, m/z = 1621.35 $[M\text{-}Cl]^+$ confirmed the proposed structure, respectively. On the other hand, the $[(M\text{-}4I)/4]^+$ signals were observed at 421.12 $[(M\text{-}4I)/4]^+$, 422.24 $[(M\text{-}4I)/4]^+$ and 420.12 $[(M\text{-}Cl\text{-}4I)/4]^+$ in mass spectra, supported the proposed structures of water-soluble (**3a, 4a, 5a**), respectively. The electronic absorption spectra of (**3, 4, 5**) and (**3a, 4a, 5a**) in DMF at room temperature are shown in Figure 3. As shown in Figure 3, the Q bands were observed as single and narrow bands at ~1x10^{-5} M. These bands confirm the monomeric behavior of the metallophthalocyanines (MPcs). The absorption spectra of (**3, 4, 5**) and (**3a, 4a, 5a**) displayed Q bands at 668, 680, 729, 671, 680, 728 nm, respectively. The B (Soret) bands of (**3, 4, 5**) and (**3a, 4a, 5a**) were observed at 328, 341, 355, 327, 345, 367 nm, respectively. All spectral data confirmed the suggested structure of cobalt(II), copper(II), and manganese(III) phthalocyanines (**3, 4, 5**) and their water-soluble derivatives (**3a, 4a, 5a**).

3.2. Inhibition study of α-glucosidase

In this study, in vitro anti-α-glucosidase effects the compounds **3a, 4a, 5a** were investigated by spectrophotometric methods. Acarbose was used as a positive control. The results were tabulated as IC_{50} values in Table 1. All of the compounds showed higher inhibitory effects on α-glucosidase than that of acarbose (IC_{50} = 60.28 ± 3.42 μM). **4a** has the best inhibitory actions with 1.36 ± 0.01 μM of IC_{50} value among the tested compounds. **4a** and **5a** had an inhibitory activity about 40 times higher inhibitory activity than that of acarbose. According to the literature, Güzel et al. investigated inhibitory effects of peripheral furan-2-ylmethoxy-substituted copper and manganese phthalocyanines on α-glucosidase [26]. The IC_{50} values of these compounds were determined as 911.20 μM and 695.37 μM, respectively. The peripherally tetra-({6-[3-(diethylamino)phenoxy]hexyl}oxy substituted cobalt(II), copper(II), manganese(III) phthalocyanines displayed a higher inhibitory effect on α-glucosidase than that of furan-2-ylmethoxy-substituted compounds on α-glucosidase, according to the IC_{50} values.

In this work, Lineweaver-Burk and Dixon plots were investigated to evaluate the inhibitory type and inhibition constant (K_i) for **4a** which had the best inhibitory actions on α-glucosidase. The results are given in Table 2 and Figure 4. On enhancing substrate and inhibitors concentrations against α-glucosidase, V_{max} (maximum rate) value diminished and K_m value increased. This result claimed that the compound inhibited the enzyme via mixed inhibition.

3.3. Inhibition studies of AChE and BuChE

The in vitro antiChEs actions of all synthesized compounds were investigated to determine their therapeutic potential in AD. Galantamine was used as a positive control. The results are shown in Table 3. The results showed that the compounds have higher inhibition efficiency on AChE and BuChE when compared to galantamine (IC_{50} = 30.20 ± 0.58 μM for AChE and 52.04 ± 0.55 μM for BuChE). The IC_{50} values of **3a, 4a, 5a** were 0.65 ± 0.01 μM, 1.08 ± 0.03 μM, and 1.35 ± 0.01 μM,

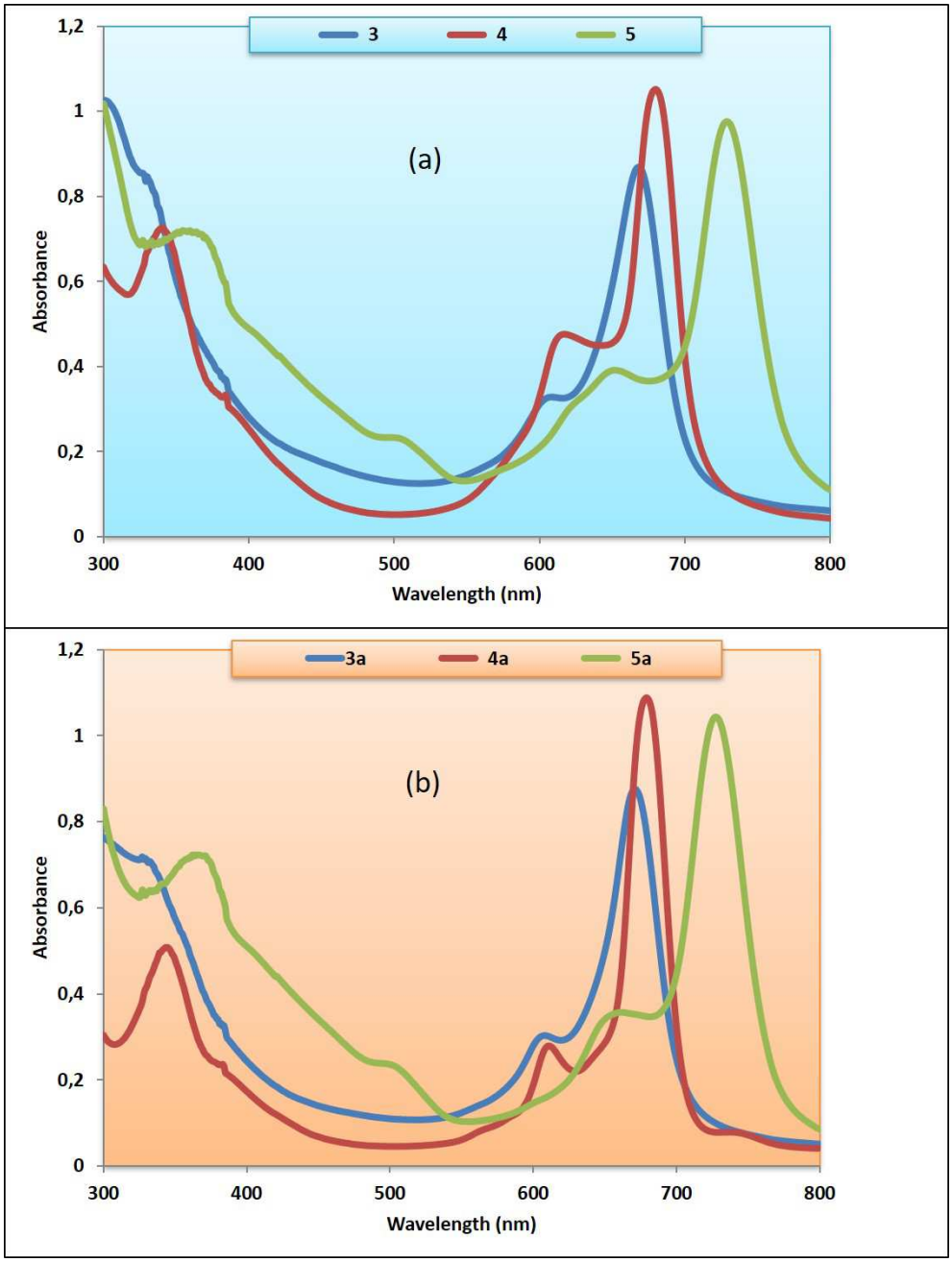

Figure 3. UV-vis spectra of **3, 4, 5** (a) and **3a, 4a, 5a** (b) in DMF.

Table 1. IC_{50} values of the compounds on α-glucosidase.

	α-Glucosidase
3a	2.48 ± 0.04***
4a	1.36 ± 0.01***
5a	1.49 ± 0.02***
Acarbose	60.28 ± 3.42

*** $p < 0.0001$ vs. positive control

Table 2. Kinetic parameters of the compounds on AChE, BuChE, and α-glucosidase.

	α-Glucosidase		AChE		BuChE	
	Type	K_i	**Type**	K_i	**Type**	K_i
3a	-	-	competitive	0.51 ± 0.04	-	-
4a	mixed	0.49 ± 0.03	-	-	mixed	0.05 ± 0.01

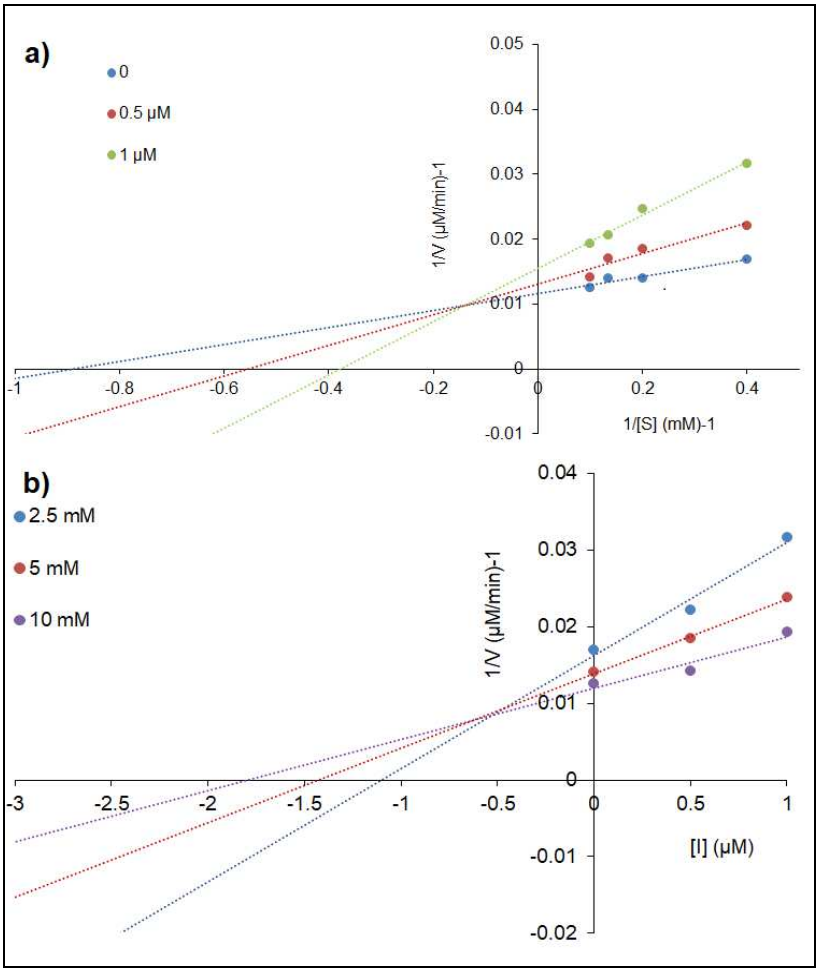

Figure 4. Lineweaver-Burk (a) and Dixon (b) plots of **4a** on α-glucosidase.

Table 3. IC_{50} and SI values of the compounds on AChE, BuChE.

	AChE	**BuChE**	**SI values (BuChE/AChE)**
3a	0.65 ± 0.01***	3.06 ± 0.02***	4.70
4a	1.08 ± 0.03***	0.29 ± 0.01***	0.27
5a	1.35 ± 0.01***	3.57 ± 0.03***	2.42
Galantamine	30.20 ± 0.58	52.04 ± 0.55	1.72

*** $p < 0.0001$ vs. positive control

respectively on AChE. In addition, the compounds displayed significant BuChE inhibitory properties that of galantamine ($p < 0.0001$). **4a** had the best BuChE inhibitory actions with 0.29 ± 0.01 μM of IC_{50} value following **3a** with 3.06 ± 0.02 μM of IC_{50} value. According to the SI (selective index (IC_{50} = BuChE/IC_{50} = AChE)) values, **3a** inhibited AChE selectively (SI value = 4.70). The difference in the results is thought to be due to the metal effect. Frasco et al. reported the metals inhibitory effects of different metals (copper, nickel, zinc, cadmium, and mercury) on AChE [34]. The results showed that copper, zinc, cadmium, and mercury inhibited on AChE [34].

In literature, Arslan reported novel peripherally tetra-chalcone substituted metal-free, manganese, cobalt and copper phthalocyanines and their inhibitory effects against AChE [34]. These compounds had lower inhibitory effects than neostigmine (IC_{50} = 0.136 ± 0.011 μM) which was used as a positive control but **3a** showed higher inhibitory actions about 46 times than galantamine on AChE [35]. In our previous study, the ChEs inhibitory effects of peripheral or nonperipheral tetra-[4-(9H-carbazol-9-yl)phenoxy] substituted cobalt, manganese phthalocyanines were investigated and IC_{50} values of these compounds were determined ranging from 7.39 ± 0.25 μM to 58.02 ± 4.94 μM [36]. The compounds used in this study were found to be more effective when compared to our previous study according to the IC_{50} values [36].

In kinetic analysis, **3a** showed competitive inhibition with V_{max} unchanged and K_m increased on AChE, according to the Lineweaver-Burk plot (Figure 5a). On the other hand, **3a** was a mixed inhibitor due to the change of V_{max} and K_m values toward BuChE (Figure 6a). K_i values of the compounds were determined as 0.51 ± 0.04 μM for **3a** and 0.05 ± 0.01 μM for **4a**, respectively (Figures 5b and 6b).

4. Conclusion

In this work, we have synthesized and characterized peripherally tetra-({6-[3-(diethylamino)phenoxy]hexyl}oxy) substituted metallophthalocyanines (**3, 4, 5**) and their water-soluble derivatives (**3a, 4a, 5a).** Also, we have reported

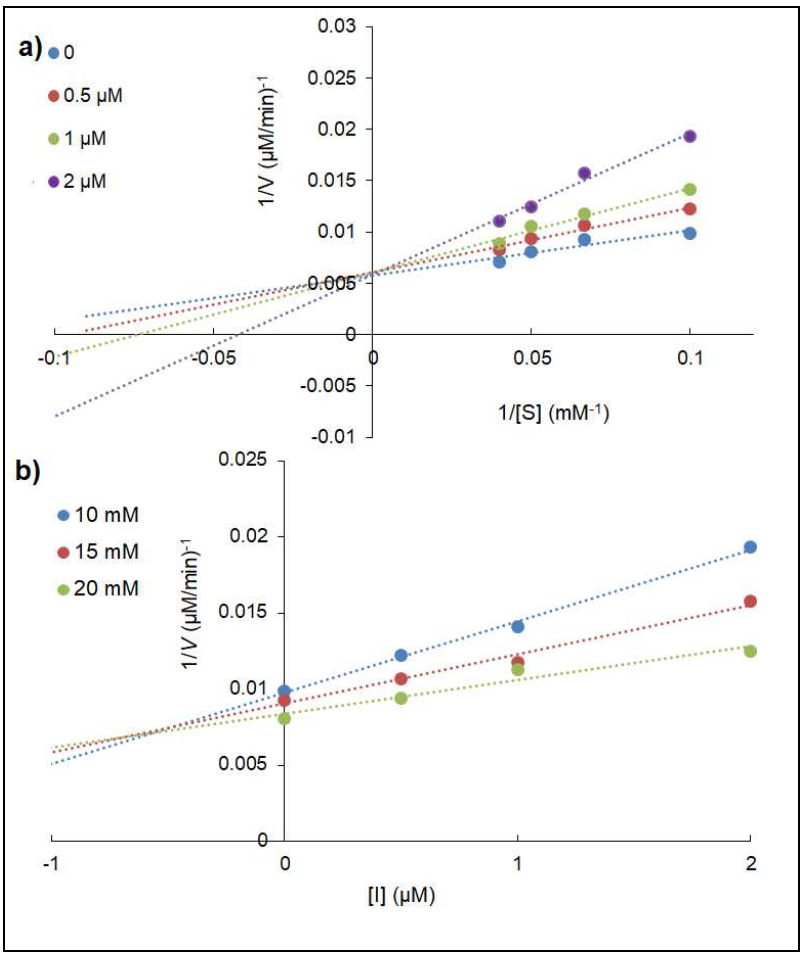

Figure 5. Lineweaver-Burk (a) and Dixon (b) plots of **3a** on AChE.

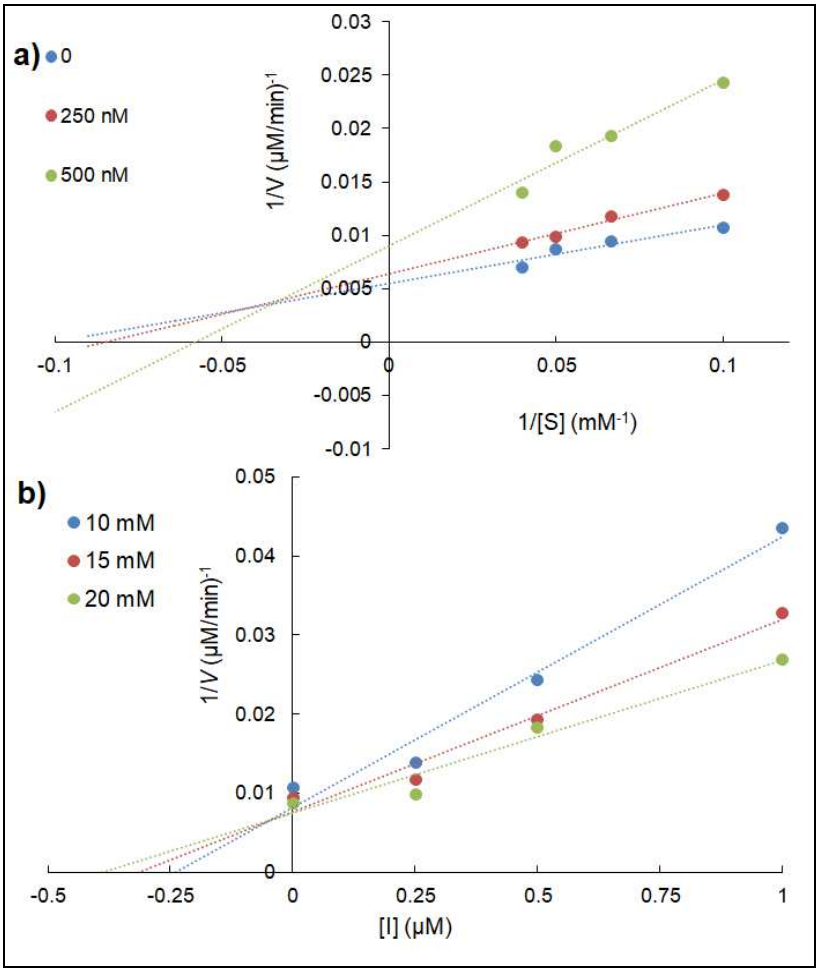

Figure 6. Lineweaver-Burk (a) and Dixon (b) plots of **4a** on BuChE.

α-glucosidase and ChEs inhibitory actions of **3a, 4a, 5a** using spectrophotometric methods. All compounds had significant inhibitory properties on α-glucosidase and ChEs. According to the IC_{50} values, **4a** had the highest inhibitory effects among the tested compounds against α-glucosidase. **4a** and **5a** showed 40 fold higher inhibitory effects than acarbose. In ChEs studies, the compounds had significant inhibitory actions when compared to galantamine ($p < 0.0001$). **3a** inhibited the AChE enzyme selectively, according to the SI value. In kinetic studies, **4a** was a mixed inhibitor for α-glucosidase, **3a** was a competitive inhibitor for AChE, and **4a** was a mixed inhibitor for BuChE. Although it has been determined that these compounds have potential against DM and AD treatments in vitro, these data should be supported by further studies.

Acknowledgment
This study was not supported by any organization.

References

1. Chen SD, Yong TQ, Xiao C, Gao X, Xie YZ et al. Inhibitory effect of triterpenoids from the mushroom Inonotus obliquus against α-glucosidase and their interaction: Inhibition kinetics and molecular stimulations. Bioorganic Chemistry 2021; 115: 105276.

2. Tian JL, Si X, Wang YH, Gong ES, Xie X et al. Bioactive flavonoids from Rubus corchorifolius inhibit α-glucosidase and α-amylase to improve postprandial hyperglycemia. Food Chemistry 2021; 341: 128149.

3. Sherafati M, Mirzazadeh R, Barzegari E, Mohammadi-Khanaposhtani M, Azizian H et al. Quinazolinone-dihydropyrano [3, 2-b] pyran hybrids as new α-glucosidase inhibitors: Design, synthesis, enzymatic inhibition, docking study and prediction of pharmacokinetic. Bioorganic Chemistry 2021; 109: 104703.

4. Laakso M, Cederberg H. Glucose control in diabetes: which target level to aim for? Journal of Internal Medicine 2012; 272: 1-12.

5. Kausar N, Ullah S, Khan MA, Zafar H, Choudhary MI et al. Celebrex derivatives: Synthesis, α-glucosidase inhibition, crystal structures and molecular docking studies. Bioorganic Chemistry 2021; 106: 104499.

6. Guerrini R, Marzola E, Trapella C, Molinari S, Cerlesi MC et al. A novel and facile synthesis of tetra branched derivatives of nociceptin/orphanin FQ. Bioorganic Medicinal Chemistry 2014; 22: 3703-3712.

7. Hamed YS, Abdin M, Rayan AM, Akhtar HMS, Zeng X. Synergistic inhibition of isolated flavonoids from *Moringa oleifera* leaf on α-glucosidase activity. LWT-Food Science and Technology, 2021; 141: 111081.

8. Phan MAT, Wang J, Tang J, Lee YZ, Ng K. Evaluation of α-glucosidase inhibition potential of some flavonoids from Epimedium brevicornum. LWT-Food Science and Technology 2013: 53: 492-498.

9. Kaur R, Kumar R, Dogra N, Yadav AK. Design, synthesis, biological evaluations and in silico studies of sulfonate ester derivatives of 2-(2-benzylidenehydrazono) thiazolidin-4-one as potential α-glucosidase inhibitors. Journal of Molecular Structure 2021; 1247: 131266.

10. Saeedi M, Hadjiakhondi A, Mohammad Nabavi S, Manayi A. Heterocyclic compounds: effective α-amylase and α-glucosidase inhibitors. Current Topics in Medicinal Chemistry 2017; 17: 428-440.

11. Almaz Z, Oztekin A, Tan A, Ozdemir H. Biological evaluation and molecular docking studies of 4-aminobenzohydrazide derivatives as cholinesterase inhibitors. Journal of Molecular Structure 2021; 244: 130918.

12. Kondapalli N, Sruthi K. Novel Tacrine and Hesperetin analogues: Design, Molecular docking and *in silico* ADME studies to identify potential Acetyl choline esterase inhibitors for Alzheimer's disease. Journal of Faculty of Pharmacy of Ankara University 2020; 44: 18-32.

13. Haroon M, Khalid M, Shahzadi K, Akhtar T, Saba S et al. Alkyl 2-(2-(arylidene) alkylhydrazinyl) thiazole-4-carboxylates: Synthesis, Acetyl cholinesterase inhibition and docking studies. Journal of Molecular Structure 2021; 1245: 131063.

14. Ladner CJ, Lee JM. Pharmacological drug treatment of Alzheimer disease: the cholinergi hypothesis revisited. Journal of Neuropathology Experimental Neurology 1998; 57: 719-731.

15. Taha M, Alshamrani FJ, Rahim F, Uddin N, Chigurupati S et al. Synthesis, characterization, biological evaluation, and kinetic study of indole base sulfonamide derivatives as acetylcholinesterase inhibitors in search of potent anti-Alzheimer agent. Journal of King Saud University Science 2021; 33: 101401.

16. Francis PT, Palmer AM, Snape M, Wilcock GK. The cholinergic hypothesis of Alzheimer's disease: a review of progress. Journal of Neurology Neurosurgery Psychiatry 1999; 66: 137-147.

17. Fang L, Chen M, Liu Z, Fang X, Gou S et al. Ferulic acid–carbazole hybrid compounds: combination of cholinesterase inhibition, antioxidant and neuroprotection as multifunctional anti-Alzheimer agents. Bioorganic Medicinal Chemistry 2016; 24: 886-893.

18. Mishra CB, Manral A, Kumari S, Saini V, Tiwari M. Design, synthesis and evaluation of novel indandione derivatives as multifunctional agents with cholinesterase inhibition, anti-β-amyloid aggregation, antioxidant and neuroprotection properties against Alzheimer's disease. Bioorganic Medicinal Chemistry 2016; 24: 3829-3841.

19. Göksel M, Durmuş M, Bıyıklıoğlu Z. Synthesis and photodynamic activities of novel silicon(IV) phthalocyanines axially substituted with water soluble groups against HeLa cancer cell line. Dalton Transactions 2021; 50: 2570-2584.

20. Bilgiçli AT, Bilgiçli HG, Hepokur C, Tüzün B, Günsel A et al. Synthesis of (4R)-2-(3-hydroxyphenyl)thiazolidine-4-carboxylic acid substituted phthalocyanines: Anticancer activity on different cancer cell lines and molecular docking studies. Applied Organometallic Chemistry 2021; 35: e6242.

21. Cranston RR, Vebber MC, Rice NA, Tonnele C, Castet F et al. N-type solution-processed tin versus silicon phthalocyanines: A comparison of performance in organic thin-film transistors and in organic photovoltaics. ACS Applied Electronic Materials 2021; 3: 1873-1885.

22. Canımkurbey B, Taşkan MC, Demir S, Duygulu E, Atilla D et al. Synthesis and investigation of the electrical properties of novel liquid-crystal phthalocyanines bearing triple branched alkylthia chains. New Journal of Chemistry 2020; 44: 7424-7435.

23. Akyüz D, Koca A. Phthalocyanine-aniline dyad constructed with click electrochemistry: a novel hybrid electrochromic material. Journal of Solid State Electrochemistry 2020; 24: 431-440.

24. Güzel E, Baş H, Bıyıklıoğlu Z, Şişman İ. Dye-sensitized solar cells using silicon phthalocyanine photosensitizers with pyridine anchor: preparation, evaluation of photophysical, electrochemical and photovoltaic properties. Applied Organometallic Chemistry 2021; 35: e6214.

25. Ndebele N, Mgidlana S, Nyokong T. Electrocatalytic Activity of Cobalt Phthalocyanines Revisited: Effect of the Number of Oxygen Atoms and Conjugation to Carbon Nanomaterials. Electrocatalysis 2021; 12: 499-515.

26. Güzel E, Koçyiğit ÜM, Taslimi P, Erkan S, Taskin OS. Biologically active phthalocyanine metal complexes: Preparation, evaluation of α-glycosidase and anticholinesterase enzyme inhibition activities, and molecular docking studies. Journal of Biochemical Molecular Toxicology 2021; 35: e22765.

27. Arslan T, Çakır N, Keleş T, Bıyıklıoğlu Z, Şentürk M. Triazole substituted metal-free and metallophthalocyanines and their water soluble derivatives as potential cholinesterases ınhibitors for the treatment of Alzheimer's disease: Design, synthesis, and in vitro inhibition study. Bioorganic Chemistry 2019; 90: 103100.

28. Keleş T, Barut B, Özel A, Bıyıklıoğlu Z. Design, synthesis and biological evaluation of water soluble and non-aggregated silicon phthalocyanines, naphthalocyanines against A549, SNU-398, SK-MEL128, DU-145, BT-20 and HFC cell lines as potential anticancer agents. Bioorganic Chemistry 2021; 107: 104637.

29. Atsay A, Gül A, Koçak MB. A new hexadeca substituted non-aggregating zinc phthalocyanine. Dyes and Pigments 2014; 100: 177-183.

30. Barut B, Bıyıklıoğlu Z, Yalçın CÖ, Abudayyak M. Non-aggregated axially disubstituted silicon phthalocyanines: Synthesis, DNA cleavage and in vitro cytotoxic/phototoxic anticancer activities against SH-SY5Y cell line. Dyes and Pigments 2020; 172: 107794.

31. Barut B, Yalçın CÖ, Demirbaş Ü. The water soluble Zn(II) and Mg(II) phthalocyanines: Synthesis, photochemical, DNA photodamage and PDT effects against A549 cells. Journal of Photochemistry and Photobiology A: Chemistry 2021; 405: 112946.

32. Bıyıklıoğlu Z, Çakır V, Çakır D, Kantekin H. Crown ether-substituted water soluble phthalocyanines and their aggregation, electrochemical studies. Journal of Organometallic Chemistry 2014; 749: 18-25.

33. Şen P. Yıldız SZ, Kanmazalp SD, Dege N. New Benzimidazole Substituted Cobalt and Manganese Phthalocyanines as Hydrogen Peroxide Catalysts for Laundry Bleaching. Macroheterocycles 2018; 11: 293-303.

34. Frasco MF, Fournier D, Carvalho F, Guilhermino L. Do metals inhibit acetylcholinesterase (AChE)? Implementation of assay conditions for the use of AChE activity as a biomarker of metal toxicity. Biomarkers 2005;10(5):360-75.

35. Arslan T. Design, synthesis of novel peripherally tetra-chalcone substituted phthalocyanines and their inhibitory effects on acetylcholinesterase and carbonic anhydrases (hCA I and II). Journal of Organometallic Chemistry2021; 951: 122021.

36. Barut B, Keleş T, Biyiklioglu Z, Yalçın CÖ. Peripheral or nonperipheral tetra-[4-(9H-carbazol-9-yl)phenoxy] substituted cobalt(II), manganese(III) phthalocyanines: Synthesis, acetylcholinesterase, butyrylcholinesterase, and α-glucosidase inhibitory effects and anticancer activities. Applied Organometallic Chemistry 2021; 35: e6021.

Supplementary Information

1. Materials and methods

All reagents and solvents were of reagent grade quality and were obtained from commercial suppliers. Acarbose (Sigma, A8980), acetylcholinesterase (AChE) from *Electrophorus electricus* (electric eel) (Sigma, C3389), acetylthiocholine iodide (AChI) (Sigma, A5751), butyrylcholinesterase (BuChE) from equine serum (Sigma, C1057), butyrylthiocholine iodide (BChI) (Sigma, 20820), 5,5-dithio-bis(2-nitrobenzoic)acid (DTNB) (Sigma, D8130), galantamine (Sigma, 1287755), α-1,4-glucosidase from *Saccharomyces cerevisiae* (Sigma, G5003), and p-nitrophenyl-α-glucopyranoside (4-pNPG) (Sigma, 487506) were obtained from commercial sources. The inhibitory effects of the enzymes were performed using Thermo Scientific MultiskanTM Go Microplate Spectrophotometer using a 96-well microplate reader.

2. α-Glucosidase inhibition assay

α-Glucosidase inhibition assay was performed as previously reported with some modifications [1]. Acarbose was used as a positive control, and DMSO (final concentration .8%) as blank. The compounds (50 µL) in phosphate buffer pH 6.9, α-glucosidase (100 µL, 0.5 U/mL) were added and allowed to react for 20 min in a microplate. After incubation, 4-pNPG (50 µL, 5 mM) was added and incubated for 20 min at room temperature. The absorbance was measured at 405 nm using a 96-well microplate reader. α-glucosidase inhibition percentage of the compounds was calculated using formula 1.

3. In vitro AChE and BuChE inhibition assay

The in vitro AChE and BuChE inhibition actions were measured according to our previous method with some modifications [2]. Galantamine was used as a positive control and DMSO (final concentration 0.8%) as blank. Tris-HCl buffer (50 µL, 50 mM pH 8), DTNB (125 µL, 3 mM), AChE/BuChE (25 µL, 0.2 U/mL), and the compounds were added into the plate and incubated for 15 min at room temperature. Then, 25 µL of 15 mM of the substrate (AChI/BChI) was added into the plate to begin an enzymatic reaction. The absorbance was measured at 412 nm. AChE and BuChE inhibition percentage of the compounds was calculated using the formula. Formula = % Inhibition: $((A_{control}-A)/A_{control}) \times 100$. $A_{control}$ is the activity of the enzyme without compound and A is the activity of the enzyme with compound. The inhibitory effect of the compounds was expressed as the concentration which inhibited 50% of the enzyme activity (IC_{50}).

4. Kinetic analysis

Lineweaver-Burk and Dixon plots were performed to examine kinetic parameters (inhibitory type and constant (K_i) values) of the compounds against enzymes [3,4]. The kinetic analysis was conducted by increasing substrate concentrations in the absence and presence of the compounds. The method was analyzed according to the procedures described above for α-glucosidase and cholinesterases.

5. Statistical analysis

Statistical analysis was performed using Microsoft Excel Windows 10 and GraphPad Prism 5.0. The results were expressed as mean ± standard deviation (n = 3). Statistical analysis was performed by one-way analysis of variance (ANOVA) followed by Tukey's tests.

References

1. Şöhretoğlu D, Sari S, Özel A, Barut B. α-Glucosidase inhibitory effect of *Potentilla astracanica* and someisoflavones: Inhibition kinetics and mechanistic insights through in vitro and in silico studies. International Journal of Biological Macromolecules 2017; 105: 1062-1070.
2. Barut B, Sari S, Sabuncuoğlu S, Özel A Azole antifungal compounds could have dual cholinesterase inhibitory potential according to virtual screening, enzyme kinetics, and toxicity studies of an inhouse library. Journal of Molecular Structure 2021; 1235: 130268.
3. Lineweaver H, Burk D. The determination of enzyme dissociation constant. Journal of American Chemical Society 934; 56: 658–661.
4. Butterworth P. The use of Dixon plots to study enzyme inhibition. Biochimica et Biophysica Acta (BBA) – Enzymology 1972; 289: 251-253.